CHAPTER 5 SIMULATIONS AND THE FITTING OF RELAY CHARACTERISTICS

This chapter shows that shunts can make the swing trace a non-classical locus; thus all network locations are not equally suited for detecting the out-of-step condition.

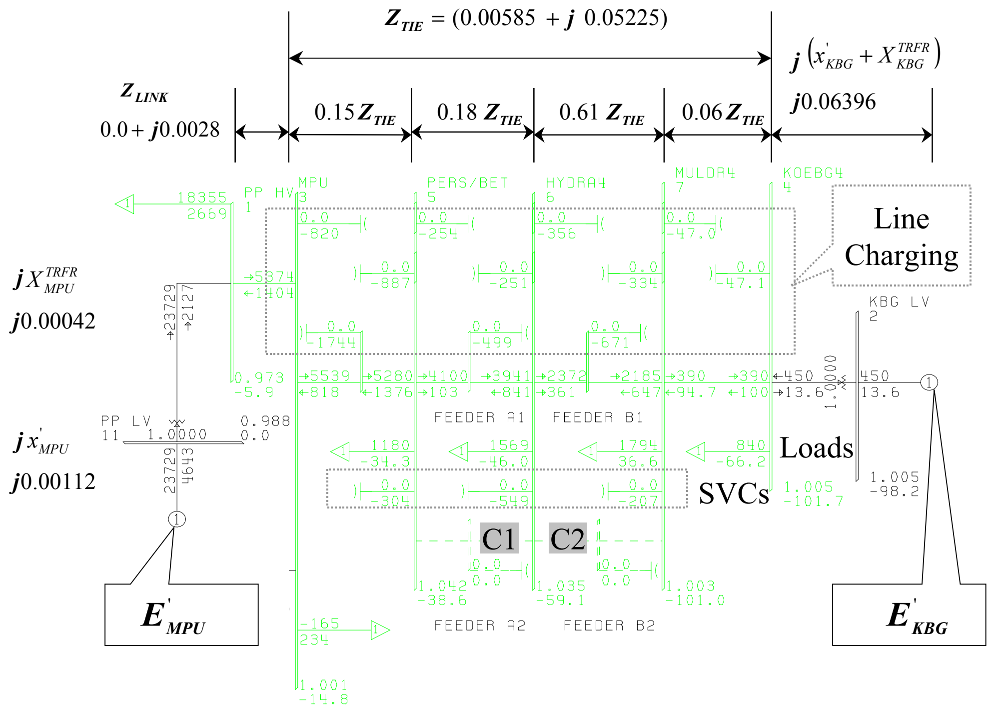

FIGURE 5.1 Steady state load flow of the improved two generator model used to model the Mpumalanga-to-Western-Cape network

The improved two generator model (Chapter 3, figure 3.25) is used to show the effect shunts have on the swing locus. The constant voltage behind transient reactance model is used to model the generators. The load is constant impedance and constant admittance shunts are used to represent the SVCs.

The effect shunts have is illustrated by showing how out-of-step polygon Z_5 is positioned to ensure Z_5 includes the impedances seen when the network loses angular stability – i.e. the impedance seen for the angles $120^{\circ} \leq \delta \leq 240^{\circ}$

(Chapter 2, section 2.11). The make up of Z_5 is shown in Chapter 2, figure 2.16, figure 2.18 and figure 2.19)

The detailed network model is used to show that locations where the swing behaves classically are the locations best suited to detect the out-of-step condition.

In the detailed network model the generators are modelled using model GENROU, the SVCs are modelled using model CSVGN1 and the loads are modelled using model CLOAD.

Figure 5.1 shows the locations C1 and C2 for which the impedance locus is constructed.

5.1 LESSONS LEARNT FROM THE IMPROVED TWO GENERATOR MODEL

5.1.1 Swing can behave non-classically

The impedance locus the swing traces is symmetrical around the network impedance $\boldsymbol{Z_Y}$ (Chapter 2, figure 2.5).

In the classical two generator model, $\boldsymbol{Z_Y}$ is approximately the line impedance of the tie line linking Gen A with Gen B.

The resistance to reactance ratio of the line that makes up the tie line of the improved two generator model is $R_{TIE}/X_{TIE} = (3/2)\times 0.07463 = 0.11195$ (Appendix B, equation B.11).

The impedance locus the improved two generator model traces at C1 is not symmetrical about the line $R_{TIE}/X_{TIE} = 0.11195$ (figure 5.2). Hence, the swing locus shown in figure 5.2 behaves non-classically.

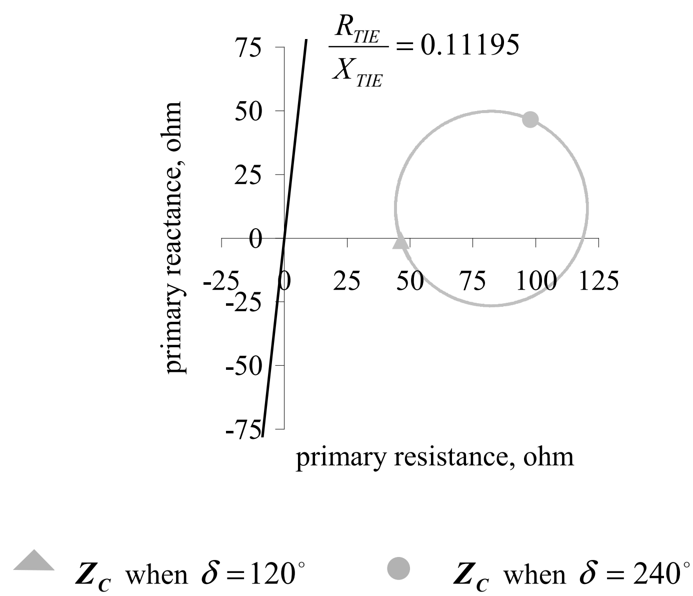

FIGURE 5.2 Impedance locus the improved two generator model traces when the network shunts are modelled. The out-of-step relay is situated at the location marked C1 in figure 5.1

5.1.2 Non-classical behaviour due to shunts

When all the shunts are removed the impedance locus the improved two generator model traces at C1 behaves classically. This is based on the fact that the impedances seen when $\delta = 120^\circ$ and when $\delta = 240^\circ$ are symmetrical about the line impedance (figure 5.3). The complete impedance locus the swing traces during the first slip cycle is shown in figure 5.4.

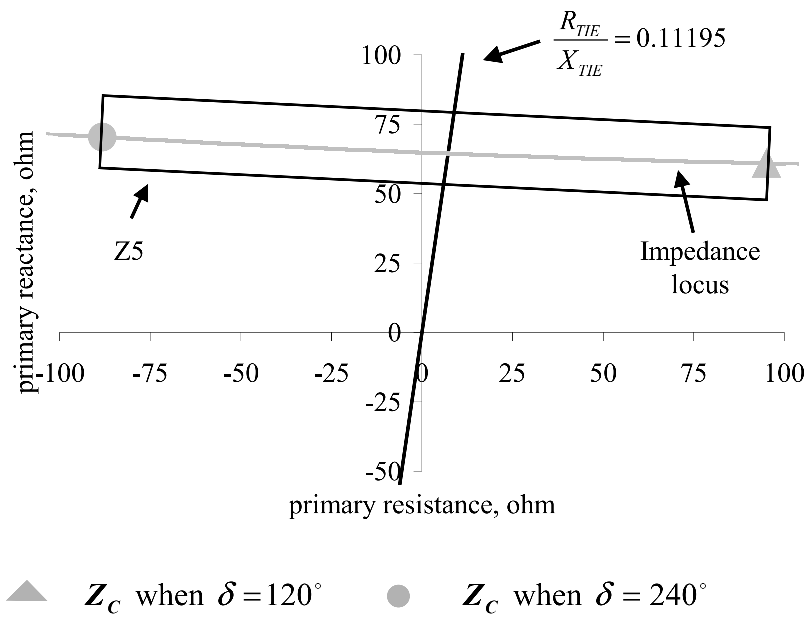

FIGURE 5.3 Z_5 has a classical complex plane position (refer to Chapter 2, figure 2.19) when the shunts are not modelled. The out-of-step relay is situated at the location marked C1 in figure 5.1

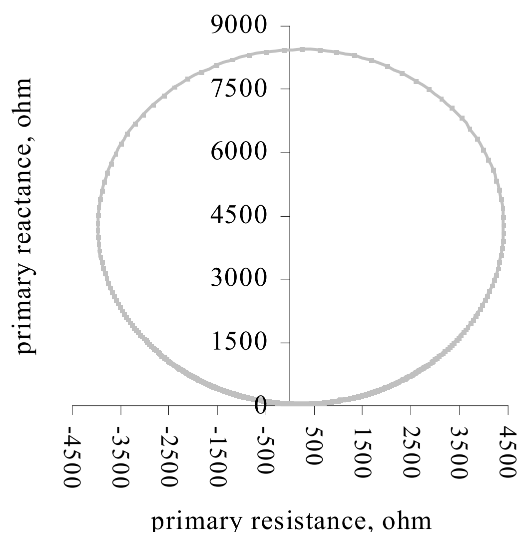

FIGURE 5.4 Impedance locus the improved two generator model traces when all the shunts are removed. The out-of-step relay is situated at the location marked C1 in figure 5.1

Hence, shunts change the swing locus shown in figure 5.3 (classical swing) into the swing locus shown in figure 5.2 (non-classical swing).

5.1.3 Reason why shunts make swings behave non-classically

In reference [23] Clarke introduces a general impedance chart that can be used to determine the impedance a distance relay sees when a network that includes shunts are slipping poles. Figure 5.5 shows the general impedance chart.

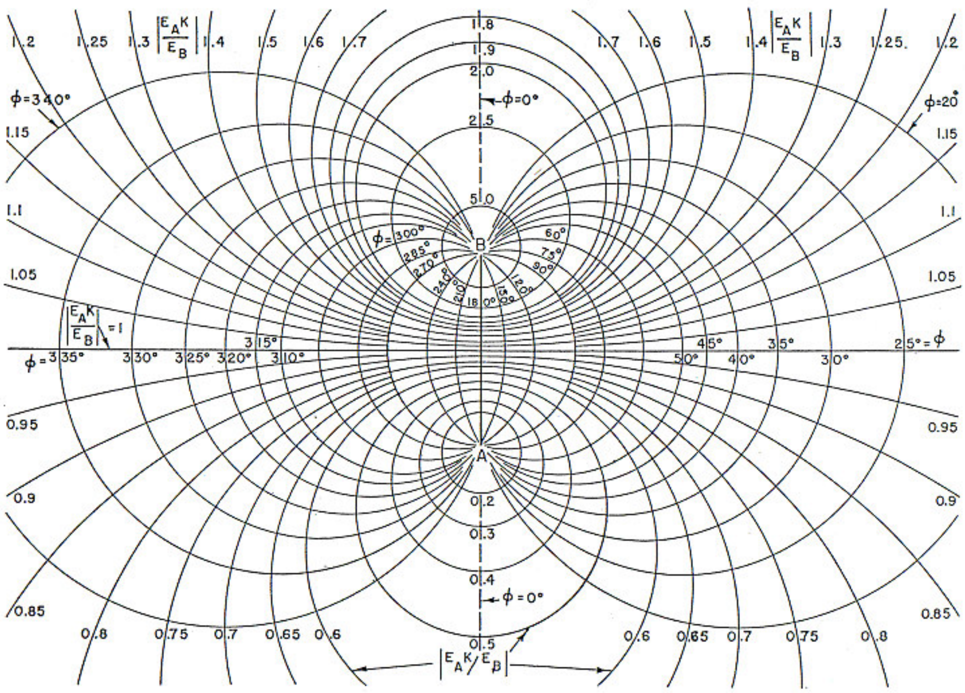

FIGURE 5.5 General impedance chart [23, p380]

The impedance locus the swing traces is symmetrical around the network impedance $\overline{\boldsymbol{AB}}$ (figure 5.5).

When no shunts are present $\overline{\boldsymbol{AB}}$ is approximately the line impedance $\overline{\boldsymbol{CD}}$ (Chapter 2, figure 2.5).

Shunts can make $\overline{\boldsymbol{AB}}$ and $\overline{\boldsymbol{CD}}$ to differ greatly. This makes the swing locus not to be symmetrical around $\overline{\boldsymbol{CD}}$. The swing then behaves non-classically.

To illustrate, we obtain the complex plane position of $\overline{\boldsymbol{AB}}$ at location C1 of the improved two generator model.

The improved two generator model includes shunts and can be separated into two parts having no connection with each other except through the relay at Point C, i.e. location C1. Hence, the improved two generator model can be simplified into the network shown in Chapter 2, figure 2.7.

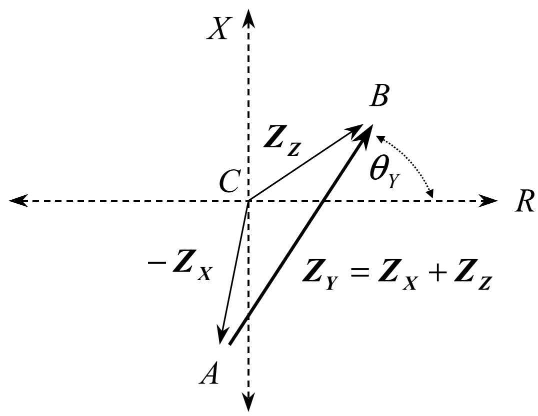

FIGURE 5.6 Position of $\overline{\boldsymbol{AB}} = \boldsymbol{Z_Y}$ in the complex plane. $-\boldsymbol{Z_X}$ locates terminal A and $\boldsymbol{Z_Z}$ locates terminal B

Point A of $\overline{\boldsymbol{AB}}$ is the impedance seen when $\boldsymbol{E}'_{\boldsymbol{A}} = 0$ and Point B of $\overline{\boldsymbol{AB}}$ is the impedance seen when $\boldsymbol{E}'_{\boldsymbol{B}} = 0$ [23, p374].

For the network shown in figure 2.7 the impedance, $\boldsymbol{Z_C}$, seen at Point C when $\boldsymbol{E}'_{\boldsymbol{A}} = \boldsymbol{E}^{\boldsymbol{TH}}_{\boldsymbol{A}} = 0$ is $-\boldsymbol{Z_X}$ (Chapter 2, equation 2.8) and the impedance seen at Point C when $\boldsymbol{E}'_{\boldsymbol{B}} = \boldsymbol{E}^{\boldsymbol{TH}}_{\boldsymbol{B}} = 0$ is $\boldsymbol{Z_Z}$ (Chapter 2, equation 2.10). The network impedance $\overline{\boldsymbol{AB}} = \boldsymbol{Z_Y}$ can be computed using $\boldsymbol{Z_Y} = \boldsymbol{Z_X} + \boldsymbol{Z_Z}$ [23, p374].

Figure 5.6 shows how $\overline{\boldsymbol{AB}}$ is positioned in the complex plane.

The condition $\boldsymbol{E}_{\boldsymbol{A}}^{'} = 0$ is simulated by replacing the Mpumalanga generator with a shunt reactor. The transient reactance of the Mpumalanga generator, expressed on a 100 MVA base, is 0.00112 p.u. (Chapter 3, equation 3.37). Therefore, the MVA rating of the equivalent reactor is:

$$Q_{MPU} = \left|\boldsymbol{V}_{\boldsymbol{MPU}}\right|^2 \times \frac{100}{0.00112}$$

$$\approx 89285.7 \text{ MVA} \tag{5.1}$$

The condition $\boldsymbol{E}_{\boldsymbol{B}}^{'} = 0$ is simulated by replacing the Koeberg generator with a shunt reactor. The transient reactance of the Koeberg generator, expressed on a 100 MVA base, is 0.05046 p.u. (Chapter 3, equation 3.32). Therefore, the MVA rating of the equivalent reactor is:

$$Q_{KBG} = \left|\boldsymbol{V}_{\boldsymbol{KBG}}\right|^2 \times \frac{100}{0.05046}$$

$$\approx 1981.8 \text{ MVA} \tag{5.2}$$

Figure 5.7 and figure 5.8 show the seen impedance when $\boldsymbol{E}_{\boldsymbol{A}}^{'} = 0$ and when $\boldsymbol{E}_{\boldsymbol{B}}^{'} = 0$.

Positive current flows from $\boldsymbol{E}_{\boldsymbol{A}}^{'}$ to $\boldsymbol{E}_{\boldsymbol{B}}^{'}$ [23, p373]. Therefore, current flowing towards Mpumalanga is negative current. Hence, the per unit impedance shown in figure 5.7 is $\boldsymbol{Z}_{\boldsymbol{X}}$ and the per unit impedance shown in figure 5.8 is $-\boldsymbol{Z}_{\boldsymbol{Z}}$.

The per unit impedances shown can be converted to actual impedances by multiplying by 1600 ohms (Appendix I, section I.1).

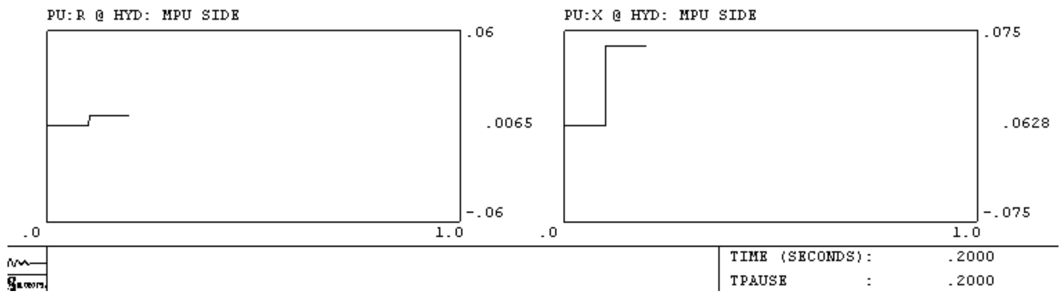

FIGURE 5.7 Value of $-\boldsymbol{Z_C}$ at C1 when $\boldsymbol{E_A^{TH}} = \boldsymbol{E_A^{'}} = 0$. Observer looks toward Mpumalanga

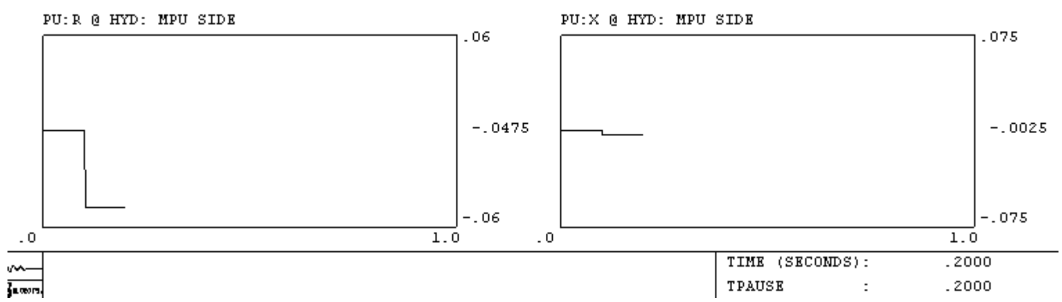

FIGURE 5.8 Value of $-\boldsymbol{Z_C}$ at C1 when $\boldsymbol{E_B^{TH}} = \boldsymbol{E_B^{'}} = 0$. Observer looks toward Mpumalanga

Figure 5.9 shows the complex plane location of the network impedance $\overline{\boldsymbol{AB}}$ at C1. Appendix J, section J.1 shows that the value we computed for $\overline{\boldsymbol{AB}}$ is correct.

$\overline{\boldsymbol{AB}}$ shown in figure 5.9 differs greatly from the line impedance that makes up the tie line of the improved two generator model. The mentioned line impedance is situated along the line $R_{TIE} : X_{TIE}$. Hence, the swing behaves non-classically at C1.

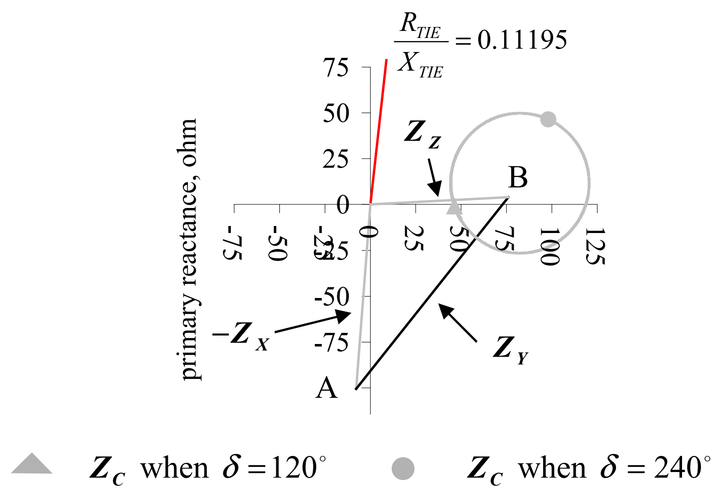

FIGURE 5.9 Complex plane position of $\overline{AB}$ at C1. $-Z_X$ locates terminal A and Z_Z locates terminal B

5.1.4 Diameter of swing locus

The diameter of the impedance locus the classical two generator model traces is determined by the source voltage ratio $\left|E'_A / E'_B\right|$ figure 5.10.

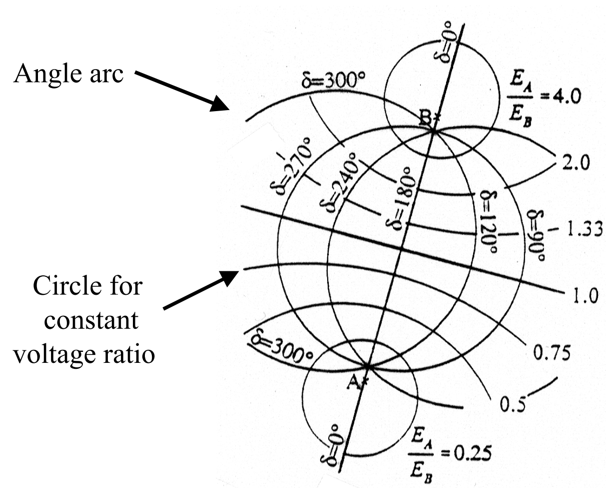

FIGURE 5.10 Impedance locus the classical two generator model traces [1, p918]

The classical approach to out-of-step relaying caters for $\left|\boldsymbol{E}_A^{'}/\boldsymbol{E}_B^{'}\right|$ to have any value between 0.87 and 1.15 (Chapter 2, figure 2.12).

When shunts are present the circles for constant voltage ratio is indexed using $\left|\left(\boldsymbol{E}_A^{'}\boldsymbol{K}\right)/\boldsymbol{E}_B^{'}\right|$ (figure 5.5). To clarify, we note Chapter 2, equation 2.7 shows the impedance seen at Point C of the network shown in figure 2.7 can be computed using:

$$\boldsymbol{Z}_C = -\boldsymbol{Z}_X + \boldsymbol{Z}_Y\left(\frac{1}{1-\boldsymbol{E}_B^{TH}/\boldsymbol{E}_A^{TH}}\right) \quad (5.3)$$

Clarke computes the impedance seen at Point C using [23, p376]:

$$\boldsymbol{Z}_C = -\boldsymbol{Z}_X + \boldsymbol{Z}_Y\left(\frac{1}{1-\boldsymbol{E}_B^{'}/\left(\boldsymbol{E}_A^{'}\boldsymbol{K}\right)}\right) \quad (5.4)$$

Setting equation 5.3 equal to equation 5.4 gives:

$$\left(\frac{1}{1-\boldsymbol{E}_B^{TH}/\boldsymbol{E}_A^{TH}}\right) = \left(\frac{1}{1-\boldsymbol{E}_B^{'}/\left(\boldsymbol{E}_A^{'}\boldsymbol{K}\right)}\right)$$

Hence:

$$\left|\frac{\boldsymbol{E}_A^{TH}}{\boldsymbol{E}_B^{TH}}\right|\angle\phi = \left|\frac{\boldsymbol{E}_A^{'}}{\boldsymbol{E}_B^{'}}\right|\angle\delta\left|\boldsymbol{K}\right|\angle\theta_k \quad (5.5)$$

Therefore, the ratio, $\left|\boldsymbol{E}_A^{TH}/\boldsymbol{E}_B^{TH}\right|$, of the Thevenin voltages seen at Point C is $\left|\boldsymbol{K}\right|$ multiplied with the ratio, $\left|\boldsymbol{E}_A^{'}/\boldsymbol{E}_B^{'}\right|$, of the source voltages of the generators.

To clarify the meaning of $\boldsymbol{K}$ the mentioned vector is computed for the network shown in Chapter 2, figure 2.6. For the network shown in figure 2.6 we have:

$$\boldsymbol{E}_A^{TH} = \boldsymbol{E}_A^{'} \frac{\boldsymbol{Z}_I}{\boldsymbol{Z}_G + \boldsymbol{Z}_I} \tag{5.6-a}$$

$$\boldsymbol{E}_B^{TH} = \boldsymbol{E}_B^{'} \frac{\boldsymbol{Z}_L}{\boldsymbol{Z}_K + \boldsymbol{Z}_L} \tag{5.6-b}$$

Hence, $\boldsymbol{E}_A^{TH} / \boldsymbol{E}_B^{TH}$ is:

$$\frac{\boldsymbol{E}_A^{TH}}{\boldsymbol{E}_B^{TH}} = \frac{\boldsymbol{E}_A^{'}}{\boldsymbol{E}_B^{'}} \left[\frac{\boldsymbol{Z}_K / \boldsymbol{Z}_L + 1}{\boldsymbol{Z}_G / \boldsymbol{Z}_I + 1} \right] \tag{5.7-a}$$

Therefore:

$$\boldsymbol{K} = \left[\frac{\boldsymbol{Z}_K / \boldsymbol{Z}_L + 1}{\boldsymbol{Z}_G / \boldsymbol{Z}_I + 1} \right] \tag{5.7-b}$$

Equation 5.7-b shows that the shunts $\boldsymbol{Z}_I$ and $\boldsymbol{Z}_L$ affect the value of $\boldsymbol{K}$ and, therefore, affect the value of $\left|\boldsymbol{E}_A^{TH} / \boldsymbol{E}_B^{TH}\right|$. Hence, $\left|\boldsymbol{E}_A^{TH} / \boldsymbol{E}_B^{TH}\right|$ can have a value that is greatly different than the expected range of values – i.e. the range $[0.87;1.15]$.

To show that $\left|\boldsymbol{E}_A^{TH} / \boldsymbol{E}_B^{TH}\right|$ can have a value that is well outside the range of expected source voltage ratios we obtain the value of $\left|\boldsymbol{E}_A^{TH} / \boldsymbol{E}_B^{TH}\right|$ at the location marked C1 in figure 5.1.

Figure 5.11 shows that $\left|\boldsymbol{E}_A^{TH} / \boldsymbol{E}_B^{TH}\right|$ has the value $3.82 \approx 1.297/0.34$ at C1. Appendix J shows that the value we obtained for $\left|\boldsymbol{E}_A^{TH} / \boldsymbol{E}_B^{TH}\right|$ is correct.

This large value of $\left|\boldsymbol{E}_A^{TH} / \boldsymbol{E}_B^{TH}\right|$ explains why the diameter of the swing locus the improved two generator model traces at C1 is small – refer to figure 5.2.

This small diameter is due to the shunts. To clarify, we note the diameter of the classical swing locus is large. In fact, for the case $\left|\boldsymbol{E}_{\boldsymbol{A}}^{'}\right| = \left|\boldsymbol{E}_{\boldsymbol{B}}^{'}\right|$ the diameter is infinite.

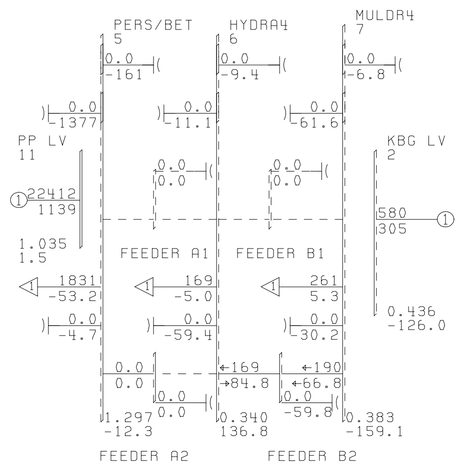

FIGURE 5.11 $\left|\boldsymbol{E}_{\boldsymbol{A}}^{\boldsymbol{TH}}\right|$ and $\left|\boldsymbol{E}_{\boldsymbol{B}}^{\boldsymbol{TH}}\right|$ on the Mpumalanga side of Hydra. The network shunts are modelled

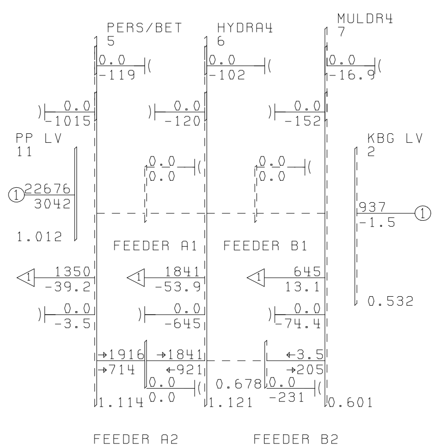

FIGURE 5.12 $\left|\boldsymbol{E}_{\boldsymbol{A}}^{\boldsymbol{TH}}\right|$ and $\left|\boldsymbol{E}_{\boldsymbol{B}}^{\boldsymbol{TH}}\right|$ on the Koeberg side of Hydra. The network shunts are modelled

The admittance of the shunt $\boldsymbol{Z_I}$ and the shunt $\boldsymbol{Z_L}$ change with network location. This affects the value of $\left|\boldsymbol{E}_A^{TH}/\boldsymbol{E}_B^{TH}\right|$. To illustrate, we obtain the value of $\left|\boldsymbol{E}_A^{TH}/\boldsymbol{E}_B^{TH}\right|$ at the location marked C2 in figure 5.1.

Figure 5.12 shows that $\left|\boldsymbol{E}_A^{TH}/\boldsymbol{E}_B^{TH}\right|$ has the value $1.65 \approx 1.121/0.678$ at C2.

The value 1.65 is smaller than the value 3.82. This explains why the diameter of the swing locus the improved two generator model traces at C2 is much larger than the diameter of the swing locus the improved two generator model traces at C1 – compare figure 5.13 with figure 5.2.

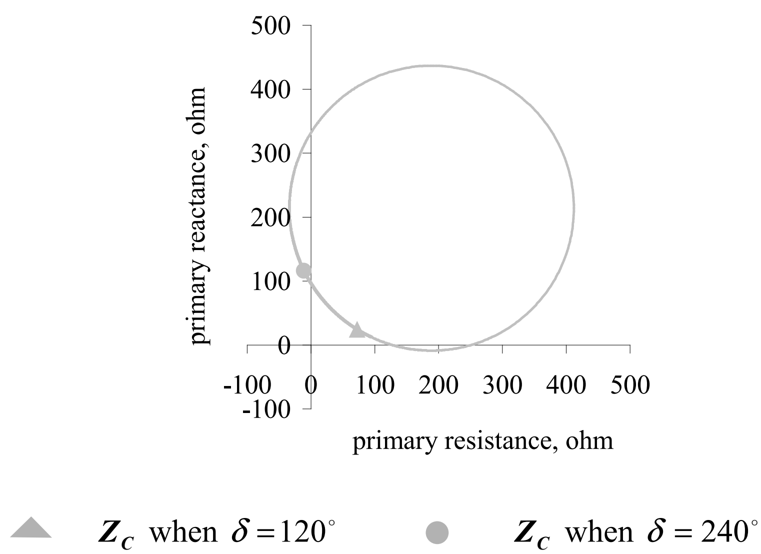

FIGURE 5.13 Impedance locus the improved two generator model traces when the network shunts are modelled. The out-of-step relay is situated at the location marked C2 in figure 5.1

5.1.5 Busbars where the swing behaves classically

Figure 5.14 shows that at location C2 the network impedance, $\overline{AB}$, is approximately situated as is shown in Chapter 2, figure 2.5. This makes the swing trace a classical locus at C2. $\overline{AB} = Z_Y = Z_X + Z_Z$ (figure 5.6).

The values of $-Z_X$ and Z_Y at C2 are shown in figure 5.15 and figure 5.16. The base impedance is 1600 ohms (Appendix I, equation I.1).

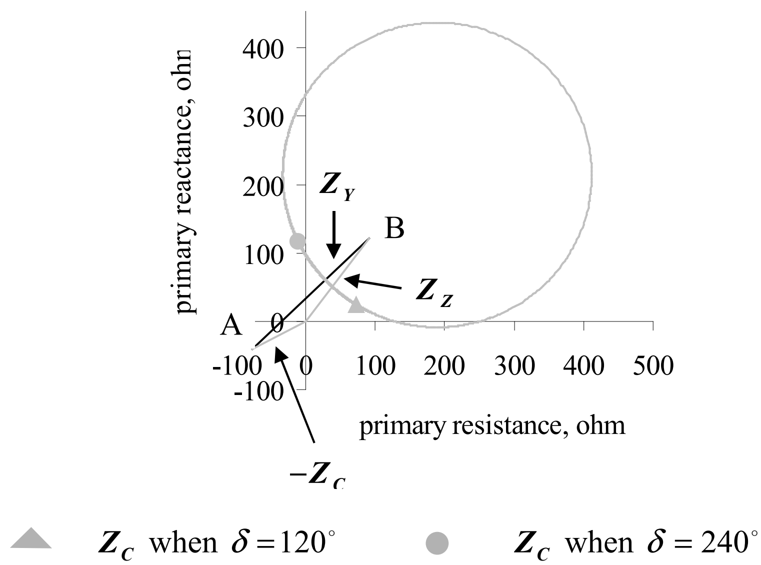

FIGURE 5.14 Complex plane position of the network impedance $\overline{AB} = Z_Y$ at the location marked C2 in figure 5.1

The impedance locus traced in figure 5.14 represents the case where the electrical centre is located between Hydra and Muldersvlei – i.e. located on the line the out-of-step relay at C2 is situated on (figure 5.17). This shows that when the swing is observed from a location that is the electrical centre the swing behaves classically.

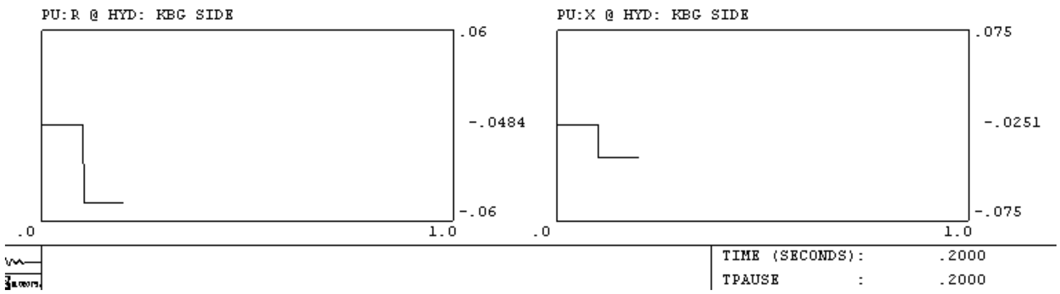

FIGURE 5.15 Value of $\boldsymbol{Z_C}$ at C2 when $\boldsymbol{E_A^{TH}} = \boldsymbol{E'_A} = 0$. Observer looks toward Koeberg

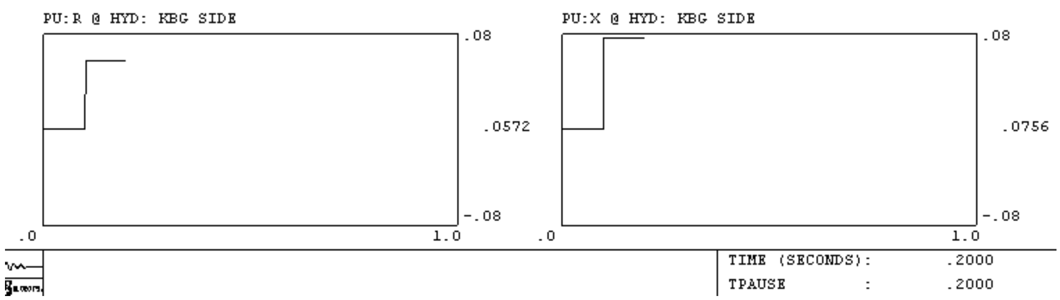

FIGURE 5.16 Value of $\boldsymbol{Z_C}$ at C2 when $\boldsymbol{E_B^{TH}} = \boldsymbol{E'_B} = 0$. Observer looks toward Koeberg

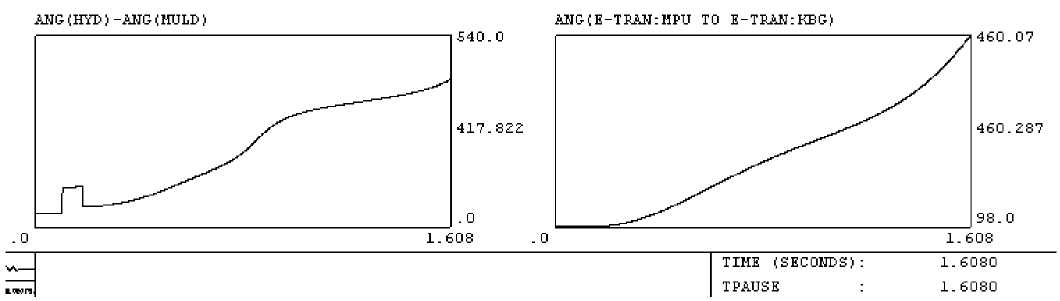

FIGURE 5.17 Power angle, δ, that develops between Hydra and Muldersvlei increases beyond 180° during the first slip cycle

5.1.6 Effect shunts have on Z_5

Figure 5.18 shows that when $\boldsymbol{Z_C}$ is viewed from a position on $\overline{\boldsymbol{AB}}$ the impedance seen when $\delta = 120^\circ$ and the impedance seen when $\delta = 240^\circ$ are mirror images. The case shown is where the classical two generator model has a source voltage ratio of $\left|\boldsymbol{E}'_A / \boldsymbol{E}'_B\right| = 1.0$.

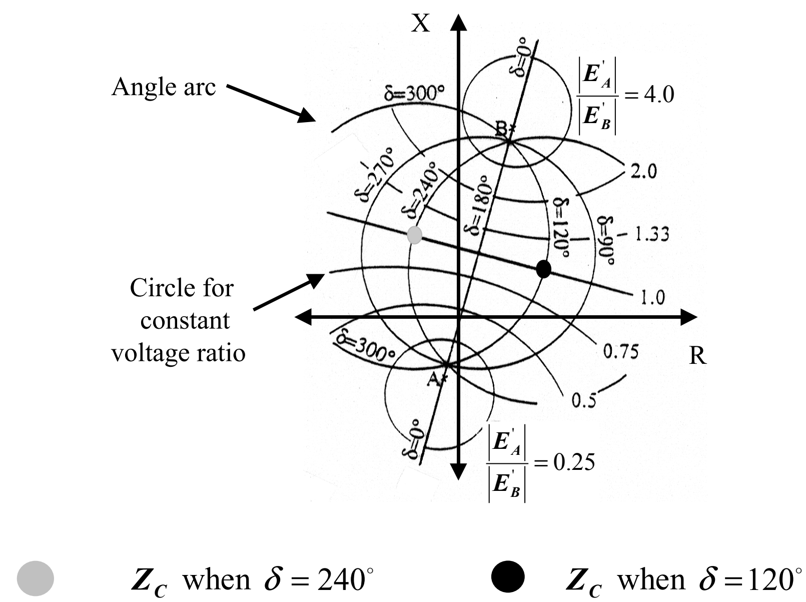

FIGURE 5.18 Impedance locus the classical two generator model traces [1, p918]

The impedance seen at C1 when $\delta = 120^\circ$ and the impedance seen at C1 when $\delta = 240^\circ$ are not mirror images (figure 5.9). This is due to shunts.

To clarify, we mark the impedance seen when $\delta = 120^\circ$ and the impedance seen when $\delta = 240^\circ$ on the general impedance chart. To mark the mentioned impedances the source voltage ratio $\left|\boldsymbol{E}_A^{TH} / \boldsymbol{E}_B^{TH}\right| = \left|\boldsymbol{E}'_A \boldsymbol{K} / \boldsymbol{E}'_B\right|$ and the angle $\phi = \delta + \theta_k$ should be known.

The value of $\left|\boldsymbol{E}_A^{TH}/\boldsymbol{E}_B^{TH}\right|$ at C1 is $\left|\boldsymbol{E}_A^{TH}/\boldsymbol{E}_B^{TH}\right| = 3.82 \approx 1.297/0.34$ (figure 5.11).

To obtain ϕ, we note that when the line current at Point C peaks, i.e. at the relay location, $\boldsymbol{E}_A^{TH}$ leads $\boldsymbol{E}_B^{TH}$ by 180 degrees. ($\boldsymbol{E}_A^{TH}$ and $\boldsymbol{E}_B^{TH}$ are the Thevenin voltages at Point C – refer to Chapter 2, figure 2.6). If δ is know when the current at Point C peaks, θ_k can be computed using:

$$\theta_k = 180^\circ - \delta \tag{5.8}$$

When the current at C1 peaks, δ has the value of $\delta = 789.45^\circ$ (figure 5.19). Hence, $\theta_k = 180^\circ - 789.45^\circ = -249.45^\circ = 110.5^\circ$.

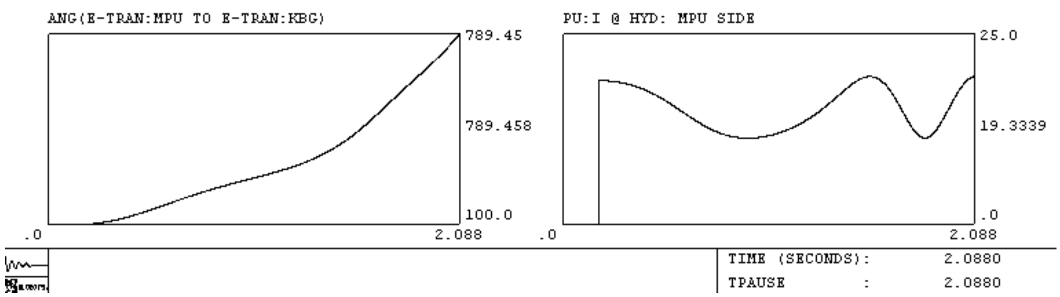

FIGURE 5.19 δ when the current at C1 peaks

Therefore, when $\delta = 120^\circ$, $\phi = 110.5^\circ + 120^\circ = 230.5^\circ$ and when $\delta = 240^\circ$, $\phi = 110.5^\circ + 240^\circ = 350.5^\circ$.

The source voltage ratio $\left|\boldsymbol{E}_A^{TH}/\boldsymbol{E}_B^{TH}\right| = 3.82$ and the angles $\phi_1 = 230.5^\circ$ and $\phi_2 = 350.5^\circ$ are not explicitly shown on the general impedance chart. However, the effect large values of $\left|\boldsymbol{E}_A^{TH}/\boldsymbol{E}_B^{TH}\right|$ and θ_k have on the impedance seen when $\delta = 120^\circ$ and $\delta = 240^\circ$ can be illustrated assuming $\left|\boldsymbol{E}_A^{TH}/\boldsymbol{E}_B^{TH}\right| = 2.5$, $\phi_1 = 240^\circ$ and $\phi_2 = 340^\circ$.

$\boldsymbol{Z}_1$ shown in figure 5.20 is the impedance seen when $\left|\boldsymbol{E}_A^{TH}/\boldsymbol{E}_B^{TH}\right| = 2.5$ and $\phi_1 = 240^\circ$. $\boldsymbol{Z}_2$ is the impedance seen when $\left|\boldsymbol{E}_A^{TH}/\boldsymbol{E}_B^{TH}\right| = 2.5$ and $\phi_2 = 340^\circ$.

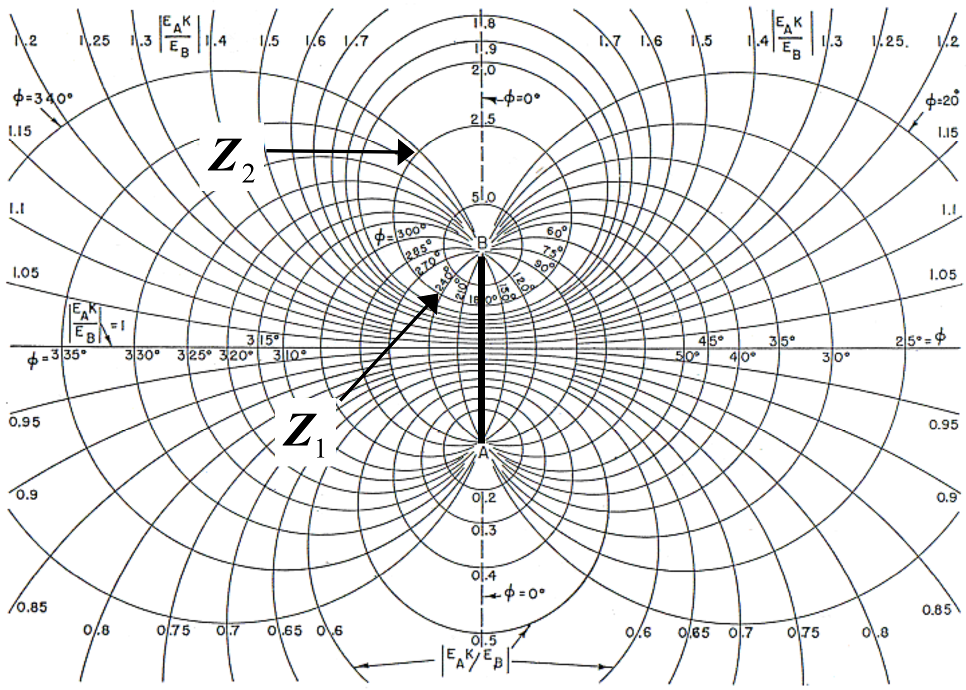

FIGURE 5.20 Marking the location of $\boldsymbol{Z}_1$ and $\boldsymbol{Z}_2$ on the general impedance chart. $\phi = \delta + \theta_k$ [23, p375]

$\boldsymbol{Z}_1$ and $\boldsymbol{Z}_2$ are not symmetrical around $\overline{\boldsymbol{AB}}$ - i.e. are not mirror images (figure 5.20). This explains why the impedance, $\boldsymbol{Z}_C^{120}$, seen at C1 when $\delta = 120^\circ$ and the impedance, $\boldsymbol{Z}_C^{240}$, seen at C1 when $\delta = 240^\circ$ are not mirror images (figure 5.9).

The fact that $\boldsymbol{Z}_C^{120}$ and $\boldsymbol{Z}_C^{240}$ are not symmetrical around $\overline{\boldsymbol{AB}}$ makes it difficult to position Z_5 using the classical approach shown in Chapter 2, figure 2.19.

To clarify, we note the classical approach positions Z_5 so that the swing locus enters Z_5 when $\delta = 120^{\circ}$ and leaves Z_5 when $\delta = 240^{\circ}$ (Chapter 2, section 2.11).

The classical approach assumes $\left|\boldsymbol{E}_A^{'}/\boldsymbol{E}_B^{'}\right|$ is approximately one for most operating conditions. To cater for abnormal operating conditions, Z_5 is positioned to border the swing lines $\left|\boldsymbol{E}_A^{'}/\boldsymbol{E}_B^{'}\right| = 0.87$ and $\left|\boldsymbol{E}_A^{'}/\boldsymbol{E}_B^{'}\right| = 1.15$ (Chapter 2, figure 2.19).

When Z_5 is positioned according to the classical approach, Z_5 will be positioned as is shown in figure 5.21.

The out-of-step characteristic the majority of commercially available out-of-step relays have can not be positioned as is shown in figure 5.21.

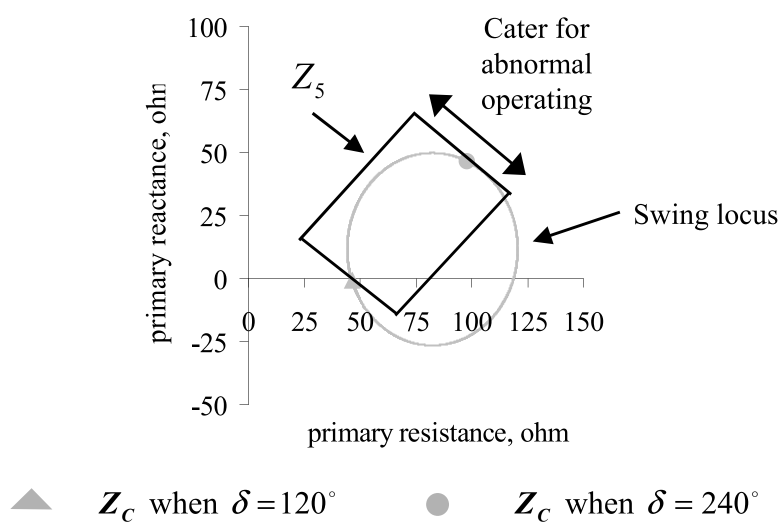

FIGURE 5.21 An illustration how to position Z_5 to ensure detection of the out-of-step condition at the location marked C1 in figure 5.1

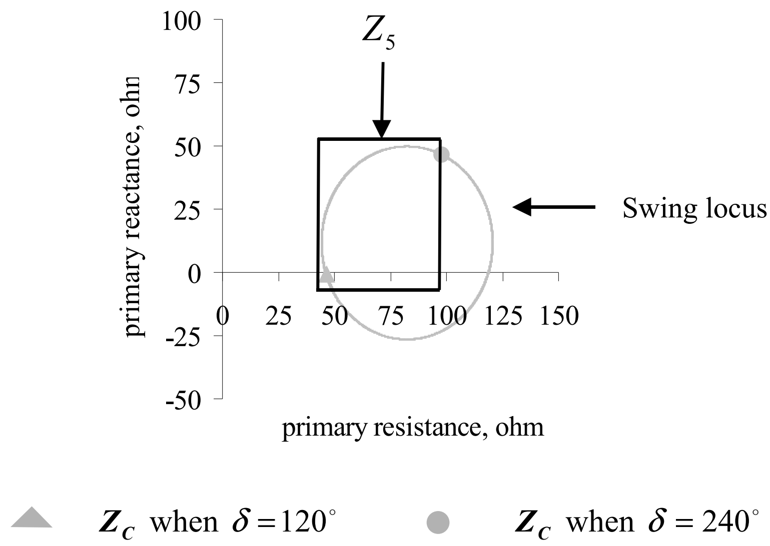

FIGURE 5.22 An illustration how to position Z_5 of the SEL 321-5 relay to ensure detection of the out-of-step condition at the location marked C1 in figure 5.1

An alternative arrangement for Z_5 is shown in figure 5.22. Z_5 of the Sel 321-5 relay can be position as is shown in figure 5.22 – refer to Chapter 2, table 2.1.

The Sel relay places polygon Z_5 within polygon Z_6 (Chapter 2, figure 2.16). This ensures that the case where the swing enters Z_5 from the bottom (figure 5.22) is catered for.

The arrangement shown in figure 5.22 leaves the impression that when the out-of-step characteristic is sufficiently flexible the swing can be detected at busbars where the swing traces a non-classical locus. However, section 5.2.1 shows that when the network load includes induction motors, the out-of-step relay at C1 can not protect the network against pole slipping.

The value of $\boldsymbol{\theta_k}$ at C2 is $\theta_k = 180^\circ - 889.2 = -349.2^\circ = 10.8^\circ$ (figure 5.23).

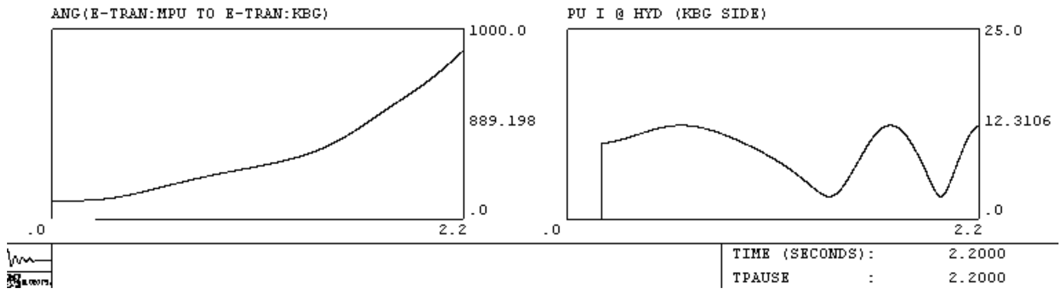

FIGURE 5.23 δ when the current at C2 peaks

The value of θ_k at C2 makes that the impedance seen at C2 when $\delta = 120^\circ$ and the impedance seen at C2 when $\delta = 240^\circ$ are symmetrical around $\overline{AB}$ - i.e. mirror images (figure 5.14). This allows Z_5 to be positioned as is shown in figure 5.24.

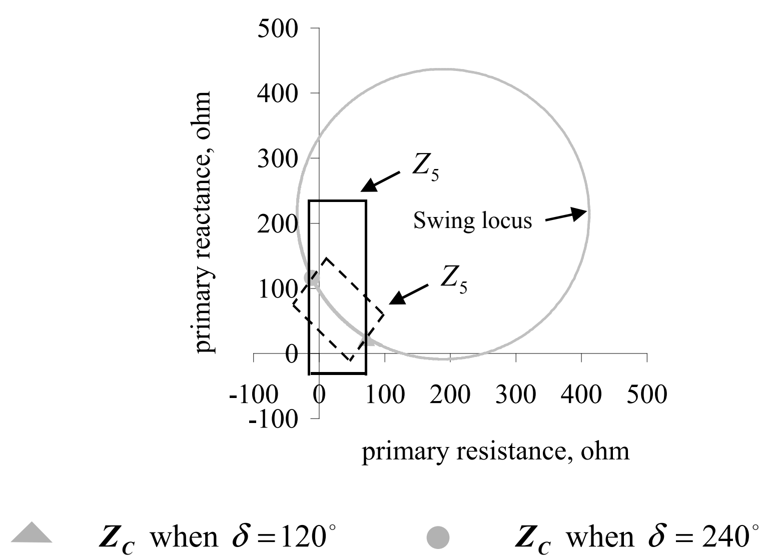

FIGURE 5.24 An illustration how to position Z_5 of the SEL 321-5 relay to ensure detection of the out-of-step condition at the location marked C2 in figure 5.1

When a SEL 321-5 relay is installed at C2, Z_5 will have the position shown in solid lines. When Z_5 is positioned according to the classical approach, Z_5 will have the position shown in dashed lines.

The characteristic of the majority of commercially available out-of-step relays can be positioned as is shown in figure 5.24.

5.1.7 Relay manual description of the out-of-step condition

The section "Out-Of-Step Logic Settings Example" of the SEL Application Guide [39] uses the classical two generator model shown in figure 5.25 when illustrating how to calculate out-of-step settings.

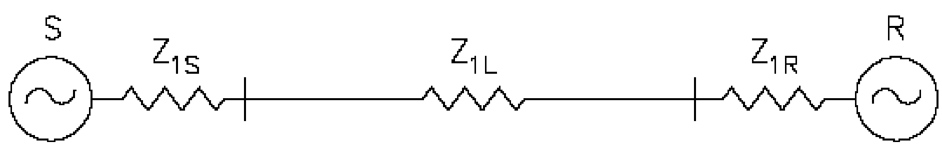

FIGURE 5.25 Network SEL Application Guide uses to illustrate the calculation of out-of-step settings [39, p8]

Figure 5.26 shows how the General Electric Company uses the classical two generator model when illustrating the typical placement of the out-of-step characteristics in the complex plane.

It follows from figure 5.25 and figure 5.26 that relay manuals do not consider the effect shunts could have on the impedance locus the swing traces.

Section 5.1.3 and 5.1.4 shows that shunts could greatly affect the impedance locus the swing traces. Hence, relay manuals over-simplify the out-of-step phenomena.

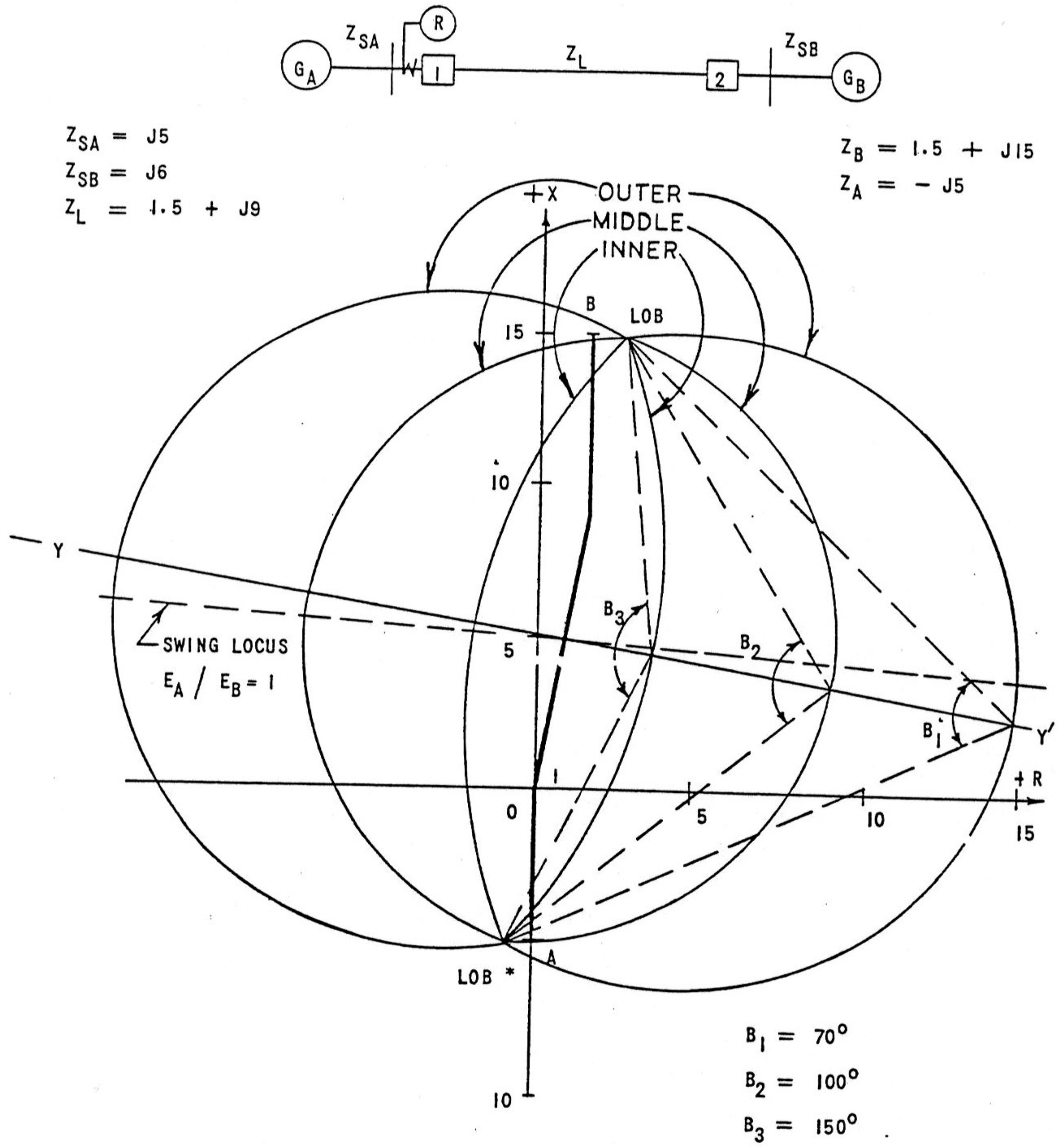

FIGURE 5.26 Typical arrangement of the out of step characteristics [9, p33]

5.2 LESSONS LEARNT FROM THE DETAILED MODEL

5.2.1 Placing out-of-step relays

The busbar best suited for detecting the out-of-step condition is the busbar where the swing traces approximately the same impedance locus for different network conditions.

To illustrate, we plot the impedance locus the detailed network model traces at Hydra obtained for the case where the generators are modelled using model GENROU, the SVCs are modelled using model CSVGN1 and the loads are modelled using model CLOAD.

Three cases are considered. All the cases weaken the network as discussed in Chapter 3, section 3.3 and use the same network load.

Case 1 uses the load mix listed in Chapter 4, table 4.2 – i.e. uses the load mix the network has at the peak of a typical winter weekday.

Case 2 uses the load mix listed in table 4.2 and loses the steam power into the Koeberg generator when the fault is cleared.

Case 3 assumes the network loses angular stability on a Sunday afternoon. This dissertation assumes 25 percent of small industrial motor load is then switched off, 50 percent of residential small motor load is then switched off and 50 percent of commercial small motor load (fans, pumps and space heating) is then switched off.

The percentage small motor load present in the network load due to industry is 28.8 percent (Appendix G, equation G.12-b). The percentage small motor load present in the network load due to residential load is 10.1 percent (Appendix G, equation G.2-b, equation G.5, equation G.6-b and equation G.8-b). The percentage small motor load present in the network load due to commercial load is 5.6 percent (Appendix G, equation G.11). Hence, to model a Sunday afternoon load 15.05 percent ($(28.8\times0.25)+(10.1\times0.5)+(5.6\times0.5)$) of the network load is moved from the “small motor” category to the “remaining” category of model CLOAD.

This dissertation assumes case 3 happens a few years after case 1 and case 2. Hence, it is reasonable to keep the network load the same – i.e. Sunday load is winter weekday load of a few years ago.

Table 5.1 lists the load components case 3 uses in the CLOAD model

The parameters CLOAD uses are listed in Chapter 4, table 4.3

Figure 5.27 shows the swing locus the detailed network model traces for each of the above cases.

Table 5.1 Load components of CLOAD

DESCRIPTION	PERCENTAGE OF BUSBAR LOAD [%]
Large motor	8.9
Small motor	38.55
Discharge lighting	12.2
Constant power	0
Remaining load	40.35

Polygon Z_5 shown in solid lines in figure 5.27 is positioned to ensure that for case 2 the impedance seen when $\delta = 120^\circ$ and $\delta = 240^\circ$ borders Z_5. This positioning of Z_5 is according to the arrangement shown in Chapter 2, figure 2.18.

The decision whether the movement in seen impedance is due to a fault, a stable or an unstable swing is made the first time the swing crosses from Z_6 to Z_5 (Chapter 2, section 2.17.1).

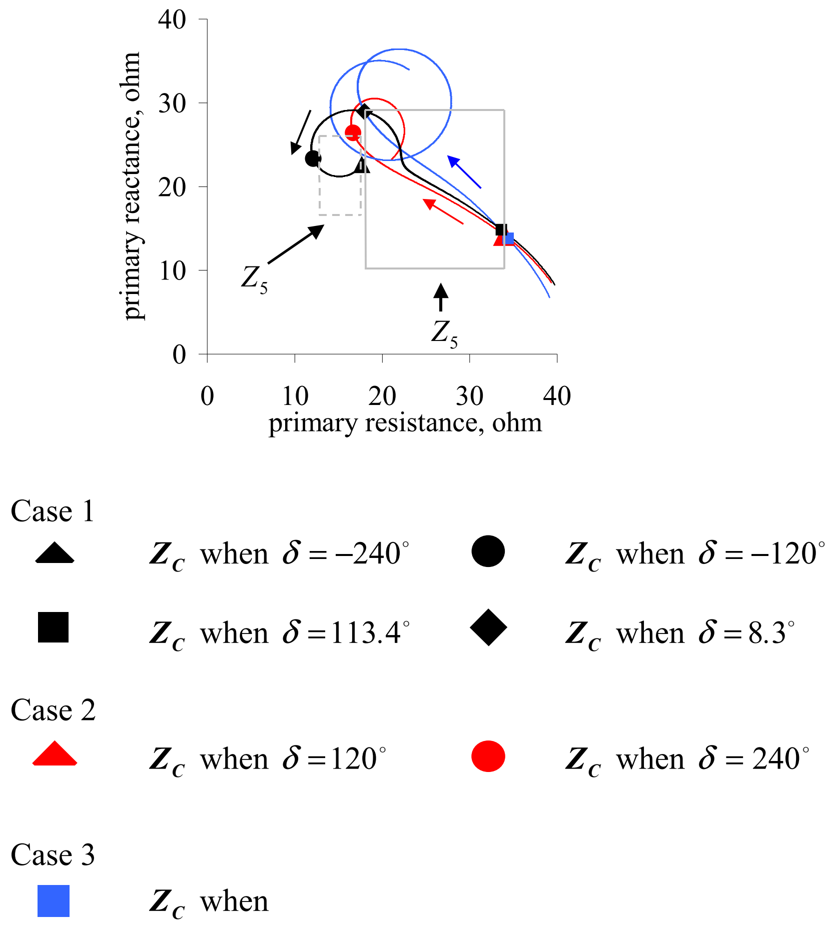

FIGURE 5.27 An illustration how to position Z_5 of the SEL 321-5 relay for the case where the out-of-step relay is situated at the location marked C1 in figure 5.1

According to Kimbark, Ravindranath and Chander, out-of-step operation is when $120^\circ \leq \delta \leq 240^\circ$ (Chapter 2, section 2.11). Hence, the first crossing of Z_5 should take place when $\delta \approx 120^\circ$. Case 1 crosses Z_5 when $\delta \approx 113.4^\circ$ and case 3 crosses Z_5 when $\delta \approx 141.9^\circ$ (figure 5.27).

The swing locus should leave Z_5 when $\delta \approx 240^\circ$. Case 1 leaves Z_5 when $\delta \approx 8.3^\circ$. This will lead to unwanted operation of the out-of-step relay.

To prevent unwanted tripping the arrangement for Z_5 shown dashed in figure 5.27 is suggested. This positioning of Z_5 does not cater for detecting the swing locus case 2 and case 3 trace. Hence, it is not possible to detect all three cases at C2.

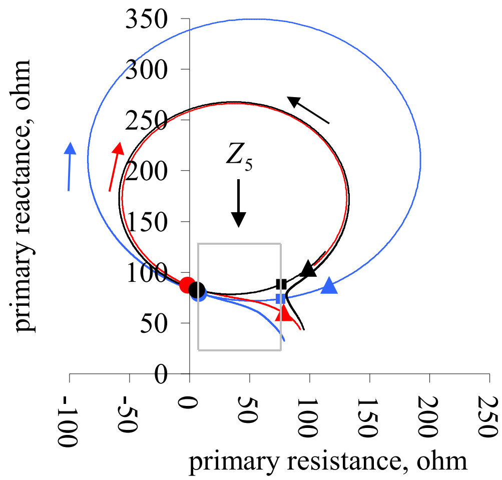

Case 1

$\boldsymbol{Z_C}$ when $\delta = -240^\circ$ $\quad$ $\boldsymbol{Z_C}$ when $\delta = -120^\circ$

$\boldsymbol{Z_C}$ when $\delta = -218.4^\circ$

Case 2

$\boldsymbol{Z_C}$ when $\delta = 120^\circ$ $\quad$ $\boldsymbol{Z_C}$ when $\delta = 240^\circ$

Case 3

$\boldsymbol{Z_C}$ when $\delta = 480^\circ$ $\quad$ $\boldsymbol{Z_C}$ when $\delta = 600^\circ$

$\boldsymbol{Z_C}$ when $\delta = 512^\circ$

FIGURE 5.28 An illustration how to position Z_5 of the SEL 321-5 relay for the case where the out-of-step relay is situated at the location marked C2 in figure 5.1

Figure 5.28 shows that all three cases can be detected at C2. To clarify, we note for case 1 the out-of-step condition is detected when $\delta = -120^\circ$. The out-of-step relay trips (TOWO) when $\delta = -218.4^\circ$ which is approximately -240°. For case 2 the out-of-step condition is detected when $\delta = 120^\circ$. The out-of-step relay trips (TOWO) when $\delta = 240^\circ$. For case 3 the out-of-step condition is detected when $\delta = 512^\circ = 152^\circ$. The out-of-step relay trips (TOWO) when $\delta = 600^\circ = 240^\circ$.

5.3 CONCLUSIONS

The accuracy with which the classical two generator model traces the actual swing locus greatly improves when the network shunts are included. This shows that shunts affect the locus the swing traces.

To clarify, we note that the detailed network model traces the impedance locus shown in figure 5.27 when the observer is situated at Hydra and looks towards Mpumalanga. The improved two generator model (i.e. classical model with the shunts included) traces a similar locus (figure 5.2). When the shunts are not included the improved two generator model traces the impedance locus shown in figure 5.3 and figure 5.4. This locus is greatly different from the locus shown in figure 5.27.

The improved two generator model is helpful in understanding the results obtained in more complex networks.

To clarify, we note that the detailed network model traces a classical locus at C2 (figure 5.28) and traces a non-classical locus at C1 (figure 5.27). The diameter of the non-classical locus is smaller than the diameter of the classical locus. The improved two generator model is helpful in showing that the effect shunts have on $\overline{\boldsymbol{AB}}$ and $\left|\boldsymbol{E}_A^{TH} / \boldsymbol{E}_B^{TH}\right|$ is the reason why the behaviour seen at C1 differs from the behaviour seen C2.

The improved two generator model should not be used to determine the optimal location of out-of-step relays.

To clarify, we note that the improved two generator model shows that it is possible to detect pole slipping by installing relays at C1 and C2 (figure 5.22 and figure 5.24). However, section 5.2.1 shows that location C1 is not suited for detecting pole slipping when the network load includes induction motors.

When shunts are located between the electrical centre and the location where the swing is observed the swing traces a non-classical impedance locus. The admittance of the shunts determines the degree of non-classical behaviour.

To clarify, we note that for the case where the Hydra load and Hydra SVC are situated between the observer and the electrical centre the swing traces a non-classical locus (figure 5.2). When the shunts situated between the observer and the electrical centre are made up of line charging the swing traces a classical locus (figure 5.14).

The busbar where the swing locus matches the classical locus best are the busbar where pole slipping should be detected.

To clarify, we note the swing locus seen at the busbars where the swing behaves classically does not change greatly when the network changes (figure 5.28). This makes it possible to determine relay settings. The swing locus seen at the busbars where the swing behaves non-classically changes greatly when the network changes (figure 5.27). This makes it difficult to obtain relay settings.

Relay manuals over-simplify the out-of-step phenomena.